

A Label-free Detection of Carcinoembryonic Antigen (CEA) using Micromechanical Biosensors

Meisam Omidi¹, Mohammadmehdi Choolaei², F. Haghirsadat¹, M. Azhdari³,
N. Davodi Moghadam⁴ and F. Yazdian¹

¹Faculty of New Science and Technology University of Tehran, Tehran, Iran

²Research Institute of Petroleum Industry (RIPI), Tehran, Iran

³Department of biochemistry, Medical University, Shahid Sadoughi University of Medical Sciences, Yazd, Iran

⁴Department of Biology, Payame Noor, Yazd, Iran

Keywords: Micromechanical Biosensors, Carcinoembryonic Antigen (CEA), Surface Stress.

Abstract: we have used arrays of micromechanical biosensors to detect carcinoembryonic antigen (CEA), a protein biomarker associated with various cancers such as colorectal, lung, breast, pancreatic, and bladder cancer. The sensing principle is based on the surface stress changes induced by antigen–antibody interaction on the micromechanical membrane (MM) surfaces. MM consists of a membrane suspended by four piezoresistive sensing components. The isotropic surface stress on the membrane results in a uniaxial stress in each sensing component, which efficiently improves the sensitivity. According to the experiments, it was revealed that MMs have surface stress sensitivities in the order of 2 (mJ/m). This matter allows them to detect CEA concentrations as low as 500 pg mL⁻¹ or 3 pM. This indicates the fact that the self-sensing MM approach is beneficial for pathological tests.

1 INTRODUCTION

The simplest micro-electromechanical systems (MEMS) structures are a new alternative technology for fabricating simple, portable, fast response and high sensitivity analytical devices for many application areas including clinical diagnosis, food quality control and environmental monitoring (Arlett 2011, Boisen et.al. 2011 and Alvarez and Lechuga 2010).

The central element in many traditional mechanical biosensors is a small cantilever that is sensitive to the biomolecule of interest. It is possible to operate micro-cantilever sensors in two different modes, i.e. cantilever bending (surface stress method) and resonance response variation (microbalance method). In the first mode, static mode, the induced surface stress that is due to the presence of the adsorbates results in a deflection in the cantilever (Wu et.al. 2001), while in the second mode, dynamic mode, the adsorbates change the resonance frequency of a cantilever due to mass loading (Omidi et al., 2013).

A sensitive readout system is crucial for

monitoring the deflection of cantilevers. For this reason several read-out methods have been presented. The most extended readout methods for biosensing are optical, and piezoresistive ones. The optical method is simple to implement and shows a linear response with sub-angstrom resolution, also is currently the most sensitive method. This method is employed for detecting the cantilever deflection in most studies (Omidi et al., 2013; Thunda et al., 1994; Lang et al., 1999 and Ghatkesar et al., 2008). Nevertheless, the optical detection mechanism presents some disadvantages for example, bulky, time-consuming laser alignment on each cantilever, low applicability for large one- or two-dimensional arrays, and the difficulty of performing measurements in opaque liquids, such as blood, may hinder the potential application of this method for actual applications.

The piezoresistive sensing method is known as a good alternative for the optical detection in biosensing application. The benefit of this method is that the principle works well in both liquid and gas phase and large arrays can be realized and read-out. Also, the technique is applicable for static as well as dynamic measurements (Mukhopadhyay et al., 2005;

Aeschimann et al., 2006; Arlett et al., 2006; Boisen and Thundat, 2009). Although piezoresistive cantilevers have proven to be highly beneficial detection methods, without effective mechanical amplification schemes, their sensitivity is far below that of optical methods. In order to overcome this problem, several researches have focused on applying structural modification, such as making a through hole, (Yu et al., 2007) patterning the cantilever surface, (Privorotskaya et al., 2008) or variation of geometrical parameters (e.g., length, width, and overall shapes) (Goericke et al., 2008 and Loui et al., 2008). Although all these methods have proven to improve the sensitivity of piezoresistive cantilevers for surface stress sensing, they have still not yielded significant stress amplification to make piezoresistive detection comparable to the optical approach, which this can be due to the fact that all these approaches rely on suppressing one of the isotropic stress components. Analytical consideration of strain amplification schemes for sensing applications based on the strategies of the constriction and double lever geometries (Yang et al., 2007) has resulted in the introduction of MMs, which have shown a considerable improvement in amplifying piezoresistive detection signals. Yoshikawa et al. (Yoshikawa et al., 2011) have experimentally evaluated a prototype nanomechanical membrane and the results have illustrated a significant sensitivity for piezoresistive cantilevers. In comparison with the standard piezoresistive cantilever, this study demonstrated a factor of more than 20 times higher sensitivity than that obtained with a standard piezoresistive cantilever.

Presently, Lung cancer, breast cancer and prostate cancer are considered as the most prevalent form of cancer in United State. Research findings indicate the importance of CEA as a useful marker for early detection of various cancers such as colorectal, lung, breast, pancreatic, and bladder cancer, monitoring patients for disease progression, and studying the effects of treatment (Brian et al. 2011 and Noelia et al., 2012). It is worth mentioning that the critical value of CEA concentration is known as 3 ng/ml.

In this study, the performance of the signal transduction biosensor was studied by using different concentrations of CEA marker in human serum albumin (HSA). A direct nano-mechanical response of micro-fabricated self-sensing MM was used to detect the surface stress changes of antigen-antibody specific binding. After injecting the CEA target, as model biocontents, the piezoresistive

responses were carefully analyzed and the feasibility of the piezoresistive membranes for biosensing were discussed in terms of device performance measures such as sensitivity, accuracy, and specificity.

2 THEORETICAL BACKGROUND

Molecular adsorptions on a surface do not only add mass, but also can induce surface tension or surface stress (Berger et al., 1997). As the molecules bind, surface stress is developed — owing to electrostatic repulsion or attraction, steric interactions, hydration and entropic effects — and this can induce deflection in the mechanical element. In the piezoresistive micro/nanomechanical sensors the electrical resistivity of a piezoresistive film varies with the applied surface stress. The resistance of the silicon piezoresistor is a function of stress and the orientation of the piezoresistors. The relation between resistivity and stress can be expressed as (Tuftte and Stelzer 1963):

$$\left[\frac{\Delta R}{R_0}\right] = \{\pi\}[\sigma] \quad (1)$$

where R_0 is the isotropic resistivity of the unstressed crystal, σ_i is the stress components, and the terms π_{ij} the component of the piezoresistance tensor. According to equation (1), for plain stress (i.e., $\sigma_z = 0$), relative resistance change can be described as follows:

$$\frac{\Delta R}{R_0} \approx \frac{\pi_{44}}{2}(\sigma_x - \sigma_y) \quad (2)$$

From equation (2), it is clear that $(\Delta R/R_0)$ is completely dependent on σ_x and σ_y values. In cantilevers sensors, surface stress induces an isotropic stress, and the piezoresistive signal is nearly zero except at the clamped end where the isotropic symmetry is broken. Thus, the sensor sensitivity efficiently reduces in comparison with cantilevers when a point force is applied at the free end. According to this problem MM approach was presented by Yoshikawa et al. (Yoshikawa et al., 2011).

A simple illustration of the final MM sensor with piezoresistive sensing component can be observed in figure 1a. Owing to equation (2), isotropic surface stress leads to zero piezoresistive signal, but in the MM structure the isotropic deformation effectively converts into a concentrated force at the connection between the membrane and the piezoresistive

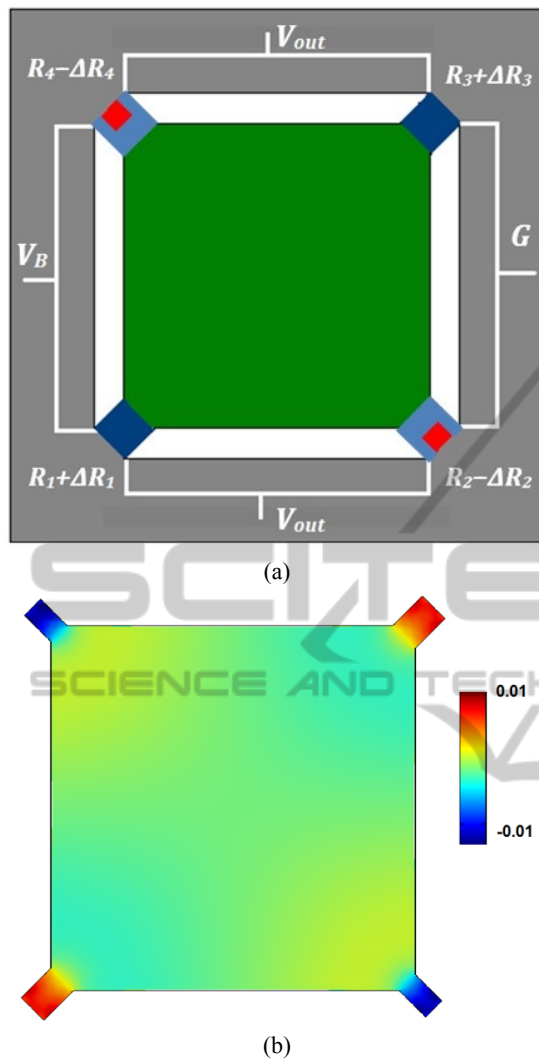


Figure 1: (a) A schematic of the MM sensor with piezoresistive sensing component (b) distribution of $\Delta R/R_0$ on the surface of MM with a dimension of $400 \mu\text{m} \times 400 \mu\text{m} \times 2 \mu\text{m}$ when a compressive surface stress of -1.0 N/m applied uniformly calculated by finite element analyses (FEA) using COMSOL Multiphysics 4.2.

sensing component. Figure 1b shows $(\Delta R/R_0)$ distribution for MM with a dimension of $400 \mu\text{m} \times 400 \mu\text{m} \times 2 \mu\text{m}$, when a compressive surface stress of -1.0 N/m is applied uniformly on the MM. COMSOL Multiphysics 4.2 finite element software was used for extracting $(\Delta R/R_0)$ distribution. The number of elements for modeling the sensor was about 25000, which gave sufficient resolution for the present simulation.

The membrane-type geometry allows us to place a full Wheatstone bridge on the chip, when all four resistors are practically equal and the relative resistance changes are small, the total output signal

V_{out} can be approximated by:

$$V_{out} = \frac{V_{in}}{4} \left(\frac{\Delta R_1}{R_1} - \frac{\Delta R_2}{R_2} + \frac{\Delta R_3}{R_3} - \frac{\Delta R_4}{R_4} \right) \quad (3)$$

According to equations (1-3), the average values of relative resistance change in the MM has a higher value in comparison with the standard cantilever (about 43 times) (Yoshikawa et al., 2011).

The intrinsic noise level for the modified piezoresistor can be estimated by Johnson (thermal) and Hooge (1/f) noise equations (Harley et al., 2000, Yu et al. 2002 and Hooge 1969). The total intrinsic noise for MM is reported as $0.01\text{--}0.5 \mu\text{V}$ (Yoshikawa et al., 2011 and 2012), which is still lower than the experimental noises ($2.0\text{--}2.5 \mu\text{V}$), mainly caused by the electrical circuit.

3 EXPERIMENTAL

3.1 Fabrication of MM Sensor

We used Silicon on Insulator (SOI) wafers with a $2 \mu\text{m}$ device layer and a $0.3 \mu\text{m}$ buried oxide (BOX) layer as the substrate material. Then a 25 nm silicon dioxide layer was grown by a thermal oxidation to electrically insulate the device layer from the subsequent metal layers. The first lithographic process to define the first metal layer for electrode and sensor platform for subsequent liftoff process has been accomplished. After patterning, the photoresist, chrome (10 nm) and gold (50 nm) layers were deposited by e-beam evaporator and patterned by a liftoff process with the previously patterned photoresist. The patterned metal layer from previous step and the patterned layer of photoresist, from the second photolithographic process were used to define the areas to be etched to define the sensor structure. The exposed device layer was etched completely by RIE to define the sensor structure. Then, a third photolithographic step for the second liftoff process, followed by the deposition of a 30-nm chrome layer and a 150-nm gold layer for wire-bonding pads. After the liftoff, a release window was photolithographically defined by the fourth lithographic process and the exposed BOX was etched by RIE leaving the Si substrate exposed. Then the wafer was diced into individual chips. Through the release window, the exposed Si substrate was etched by vapor phase etching using xenon difluoride (XeF_2) to release the sensor structure. After XeF_2 etching, the photoresist and the BOX were removed by BHF etching and solvent cleaning. The die was cleaned with oxygen plasma

and then a 100-nm thick silicon dioxide layer was deposited with plasma enhanced chemical vapor deposition (PECVD) for insulation. Chrome (20 nm) and gold (50 nm) layers were deposited using an e-beam evaporator for an immobilization layer for protein–protein interaction. The PECVD oxide on the bonding pads was selectively etched for wire-bonding. Then each die was attached to a custom made printed circuit board (PCB) and was wire-bonded. Fig. 2 presents the final picture of MM using a Scanning electron micrograph (SEM).

3.2 CEA Antibody Immobilization Process

A fresh piranha solution (a 4:1 ratio of H_2SO_4 (98.08%) and H_2O_2 (34.01%)) was used to wash and clean the membranes, in order to remove experimental contamination of the Au surface. After 1 min, the membranes were taken out of the solution and were rinsed using deionized water. To complete the cleaning process, the rinsed membranes were dried using a stream of N_2 gas. For 2 h at room temperature in darkness a 0.1 M deoxygenated cysteamine (Sigma, 95%) aqueous solution was used to functionalize the devices. Then, MMs were washed with deionized water and soaked in water for 12 h to remove the physically adsorbed cysteamine. Moreover, for creating a covalent cross-linker molecule between the amine groups on the MM surface and antibodies, chips were soaked in a 5% solution of glutaraldehyde (Sigma, 50%) in borate buffer for 2 hours. Following this and all subsequent steps, device chips were washed twice, each washing step was for two minutes, in purified DI water on an orbital shaker operating at 95 RPM. It should be mentioned that fresh water was used between washes. The reason of using water instead of buffer for washing was to prevent the abundant formation of buffer salt crystals on the surface of devices which make the sensors effectively useless. Next, one hour incubation was used to immobilize the monoclonal anti-CEA (Anti-carcinoembryonic, Sigma), affinity-purified, with a concentration of 50 mg/mL on the surface. By immersing the MM in 50 mM solution of glycine for 30 minutes unreacted glutaraldehyde was then quenched. In addition, dissolved bovine serum albumin (BSA, Sigma) in phosphate buffered saline (PBS) with 10 mg/ml concentration was used to prevent non-specific binding. For this purpose, the membranes were immersed in this solution for 1 h at room temperature. Then, they were rinsed with PBS (pH 7.4) containing polyoxyethylenesorbitan

monolaurate (Tween 20) and finally washing was performed by only using PBS solution.

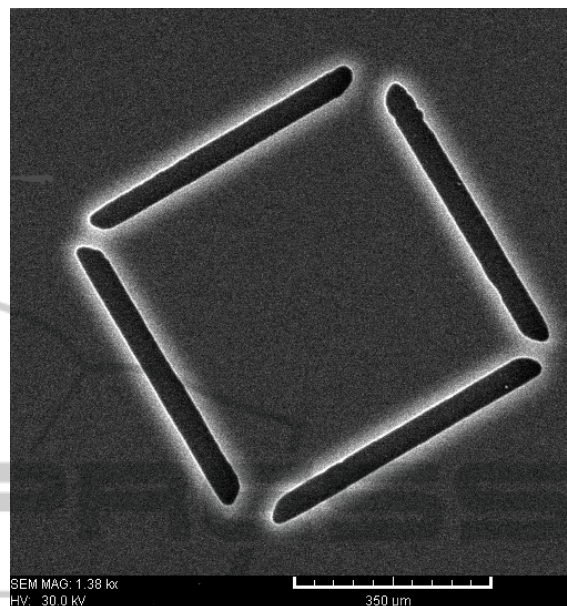


Figure 2: Scanning electron micrograph (SEM) of $400\ \mu\text{m} \times 400\ \mu\text{m} \times 2\ \mu\text{m}$ MM.

3.3 Electrical Measurements

For the electrical measurement of sensor, internal dc-bias Wheatstone bridge was used.

A bridge supply voltage of 1.5V was applied using a dc power supply (Agilent, E3631A), and the sensor output voltage was measured by a multimeter (Keithley, 2010 7-1/2). Moreover, a Faraday cage was adopted for noise reduction. The above components were used to measure the piezoresistive response of the MM in a liquid environment.

4 RESULTS AND DISCUSSION

In order to reach results with high reliability, the surfaces of the membranes were stabilized by treating them with a PBS buffer. The PBS buffer was directed with a typical flow rate of 0.4 – 0.5 ml/hour, for 1 h, to the MM sensor arrays using a flexible PDMS polymer microfluidic channel sealed to the device chip. As a general trend, at the point of initial injection of the PBS buffer the induced voltage of the MM increased rapidly and steadily decreased with time, which in this case the induced voltage of the MM reached dynamic equilibrium after 10 min. For the bio-assay, CEA antigens were injected into each liquid chamber, including the

stabilized membrane. The liquid temperature was precisely controlled and external noise sources were excluded using a shield box. In order to estimate the nonspecific adsorption on the MM surface, the concentration of HSA in all solutions was stabilized at 0.1 mg/ml.

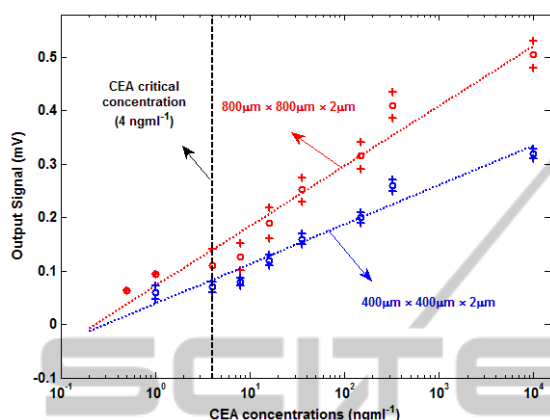


Figure 3: Steady-state output signals (V_{out}) as a function of CEA concentrations for two different MM geometries. Every data point on this plot represents an average of output signals obtained in multiple experiments done with different MM, whereas the range of output signals obtained from these experiments is shown as the error bar.

Figure 3 shows the steady-state output signals (V_{out}) as a function of CEA concentration in a HSA background for different dimensions of MM. By using a $400 \mu\text{m} \times 400 \mu\text{m} \times 2 \mu\text{m}$ MM, the lowest CEA concentration that we could clearly detect above noise was 1 ng/ml. However, when a $800 \mu\text{m} \times 800 \mu\text{m} \times 2 \mu\text{m}$ MM was used, CEA concentration as low as 0.5 ng/ml was detectable. This is close to the resolution required for CEA-based diagnosis of prostate cancer (Brian et al., 2011). The experimental results presented a range of linearity of 0.5 ng/mL to 10 $\mu\text{g/mL}$ and 1 ng/mL to 10 $\mu\text{g/mL}$ for $800 \mu\text{m} \times 800 \mu\text{m} \times 2 \mu\text{m}$ and $400 \mu\text{m} \times 400 \mu\text{m} \times 2 \mu\text{m}$ MM, respectively. The minimum detectable surface stress for each sensor can be obtained when the output signals are equal to the noise values. By using the experimental results, 2 and 3.5 mJ/m were respectively the minimum surface stress sensitivities for the $800 \mu\text{m} \times 800 \mu\text{m} \times 2 \mu\text{m}$ and $400 \mu\text{m} \times 400 \mu\text{m} \times 2 \mu\text{m}$ MM.

5 CONCLUSIONS

We have reported a novel signal transduction biosensor for detecting CEA, using a unique micro-

fabricated self-sensing array of MM sensors. Unlike cantilever sensors, which are based on optical readout systems, the MM integrated piezoresistive readout sensors facilitate the detection of compact devices in even non-transparent environments. Our unique MM design significantly improves sensor sensitivity that allows us to detect CEA concentrations as low as 500 pg/mL, or 3 pM.

REFERENCES

- Aeschimann L., Meister A., Akiyama T., Chui B. W., Niedermann P., Heinzlmann H., De Rooij N. F., Stauffer U. and Vettiger P., *Microelectron. Eng.*, 83 (2006) 1698.
- Alvarez M. and Lechuga L. M., *Analyst*, 135 (2010) 827.
- Arlett, J. L., Maloney, J. R., Gudlewski, B., Muluneh, M., Roukes, M. L. *Nano Lett.*, 6 (2006) 10 00.
- Arlett J. L., Myers E. B. and Roukes M. L., *Nat. Nanotechnol.*, 6 (2011) 203.
- Berger R., Delamarche E., Lang H. P., Gerber C., Gimezewski J. K., Meyer E. and Guntherodt, H.-J., *Science*, 276 (1997) 2021.
- Boisen A., Dohn S., Keller S. S., Schmid S. and Tenje M., *Rep. Prog. Phys.*, 74 (2011) 036101.
- Boisen A. and Thundat T., *Mater. Today*, 12 (2009) 32.
- Brian B., Shaker A M., *Nanotech. Sci. Applic*, 4 (2011) 1.
- Ghatkesar M. K., Lang H. P., Gerber C., Hegner M. and Braun T., *PLoS One*, 3 (2008) 3610.
- Goericke F. T. and King W. P., *IEEE Sens. J.*, 8 (2008) 1404.
- Guntherodt H. J., *Anal. Chim. Acta* 393 (1999) 59.
- Harley, J.A. and Kenny, T.W., *J. Microelectromech. Syst.*, 9 (2000) 226.
- Hooge, F. N., *Phys. Lett. A*, 29 (1969) 139.
- Lang H. P., Baller M. K., Berger R., Gerber C., Gimzewski J. K., Battiston F. M., Fornaro P., Ramseyer J. P., Meyer E. And Guntherodt H. J., *Anal. Chim. Acta* 393 (1999) 59.
- Loui A., Goericke F. T., Ratto T. V., Lee J., Hart B. R. and King W. P., *Sens. Actuators, A*, 147 (2008) 516.
- Mukhopadhyay R., Sumbayev V. V., Lorentzen M., Kjems J., Andreasen P. A. and Besenbacher F., *Nano Lett.*, 5 (2005) 2385.
- Noelia D., Paula D., Sergio M., María G., Sara P., Alberto O. and Manuel F., *Sens.*, 12 (2012) 2284.
- Omidi M., Malakoutian M. A., Choolaei M., *Chin. Phys. Lett.*, 30(6) (2013) 068701.
- Privorotskaya N. L. and King W. P., *Microsyst. Technol.*, 15 (2008) 333.
- Tufte O. N., and E. L. Stelzer, *J. Appl. Phys.*, 34 (1963) 313.
- Wu G., Datar R. H., Hansen K. M., Thundat T., Cote R. J. and Majumdar A., *Nat. Biotechnol.* 19 (2001) 856.
- Yang, S. M., Yin, T. I. and Chang, C. *Sens. Actuators. B*, 121 (2007) 545.

- Yoshikawa G., Akiyama T., Gautsch S., Vettiger P., and Rohrer H., *Nano Lett.*, 11 (2011) 1044.
Yoshikawa G., Akiyama T., Gautsch S., Vettiger P., and Rohrer H., *Sensors*, 12 (2012) 15873.
Yu, X. M.; Thaysen, J., Hansen, O. and Boisen, A., *J. Appl. Phys.*, 92 (2002) 6296.
Yu X. M., Tang Y. Q., Zhang H. T., Li T. and Wang W., *IEEE Sens. J.*, 7 (2007) 489.

